

Introduction to the Continuum Discretized Coupled Channels method (CDCC).

CHAU Huu-Tai Pierre

CEA, DAM, DIF F-91297 Arpajon

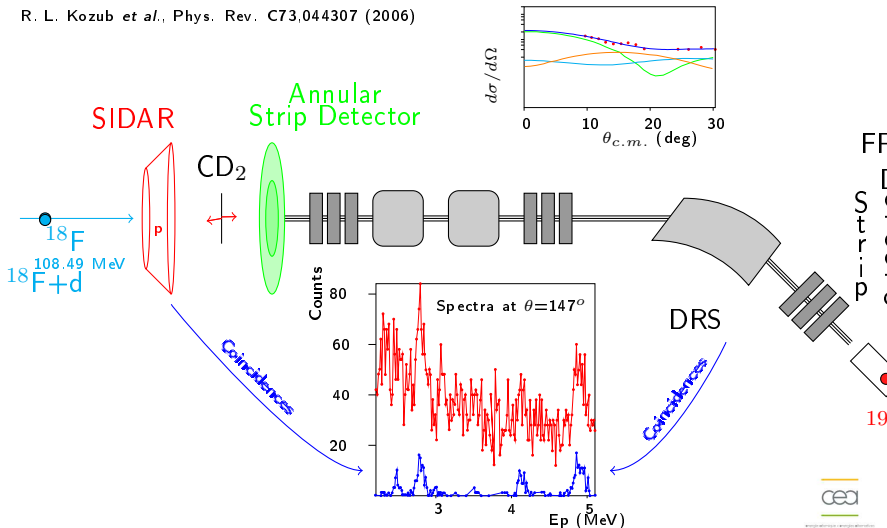
December 5-9, 2011

Contents

- 1 Introduction
- 2 The CDCC formalism.
 - References.
 - The CDCC recipes.
- 3 Applications: calculation of elastic cross section.
 - Effects of the deuteron wave function.
 - Effects of the continuum discretization.
 - Effects of the value of k_{\max} .
 - Concluding remarks.
- 4 Transfer reaction.
 - Formalism.
 - Examples.
- 5 Conclusion.
- 6 Core excitations.
 - Formalism.
 - Example of applications

Introduction: an example of (d,p) reaction.

R. L. Kozub *et al.*, Phys. Rev. C73,044307 (2006)



Introduction: what can we learn from d induced reactions?

Nuclear spectroscopy from deuteron scattering.

- ① From transfer reaction ${}^A_Z\text{X}(d,p){}^{A+1}_Z\text{X}$:
 - ① The spectrum of the nucleus ${}^{A+1}_Z\text{X}$.
 - ② The spin and parity of the levels of this nucleus.
- ② From elastic and inelastic scattering ${}^A_Z\text{X}(d,d'){}^A_Z\text{X}^*$:
 - ① The excitations energies of the nucleus ${}^A_Z\text{X}$.
 - ② The deformation parameters of this nucleus.

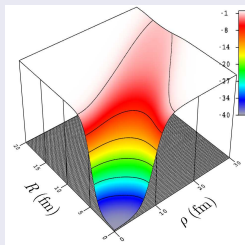
The deuteron features in the cross section calculations.

Our goal is to include the deuteron properties in the cross section calculations. We wish to take into account that the deuteron

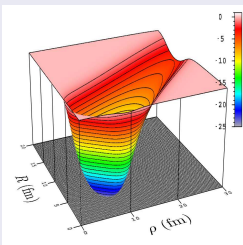
- is a **composite system**;
- and it is a **weakly bound nucleus** (low binding energy (2.2 MeV) and no excited states).

The CDCC recipes.

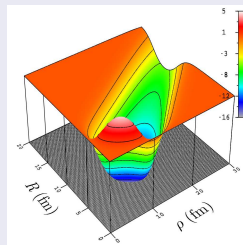
The formalism: the multipole expansion $V_{i,\lambda}(R,\rho)$.



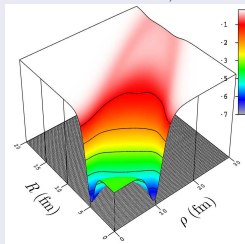
The real part of $V_{i,0}(R,\rho)$



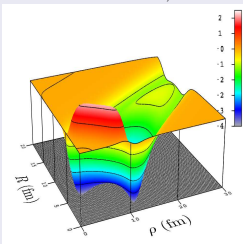
The real part of $V_{i,1}(R,\rho)$



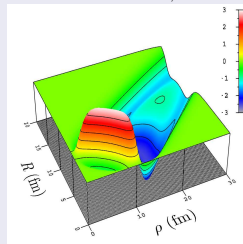
The real part of $V_{i,2}(R,\rho)$



The imaginary part of $V_{i,0}(R,\rho)$



The imaginary part of $V_{i,1}(R,\rho)$



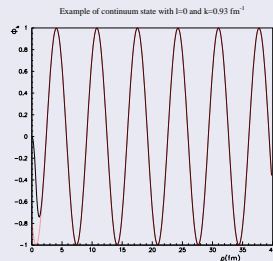
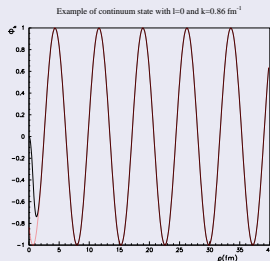
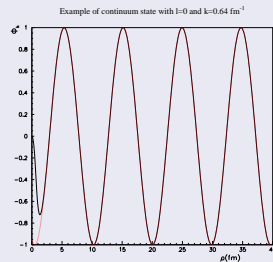
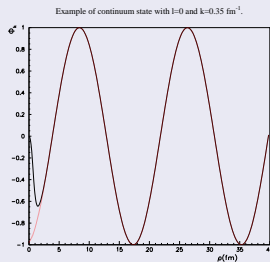
The imaginary part of $V_{i,2}(R,\rho)$

The CDCC recipes.

The formalism: the CDCC wave function.

Derivation of the $\tilde{\Phi}_j^{(2S+1)l_I; \vec{\rho}})$:
calculation of states
into the continuum.

Four examples of
continuum wave
functions (black lines)
and their asymptotic
forms (red dashed
lines) are plotted for
 $k = 0.35 \text{ fm}^{-1}$,
 $k = 0.64 \text{ fm}^{-1}$,
 $k = 0.86 \text{ fm}^{-1}$
and $k = 0.93 \text{ fm}^{-1}$.



The CDCC recipes.

The formalism: the CDCC wave function.

Derivation of the $\tilde{\Phi}_j(2S+1l_I; \vec{\rho})$: discretization by integrating over k (the average method).

Once we get the continuum states, the discretization can be performed by integrating over k within each bin $[k_i, k_{i+1}]$.
 If it is assumed that the phase shifts $\delta(l, k)$ remain constant and equal to δ then an approximation of the discretized states is given by:

$$\begin{aligned} \int_{k_i}^{k_f} \sin(k\rho + \delta)dk &= -\frac{1}{\rho} [\cos(k\rho + \delta)]_{k_i}^{k_f} \\ &= \frac{2}{\rho} \sin(\Delta k\rho) \sin(k_a\rho + \delta) \end{aligned}$$

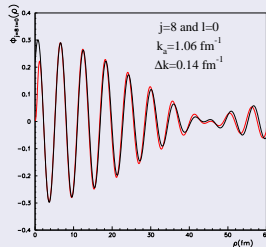
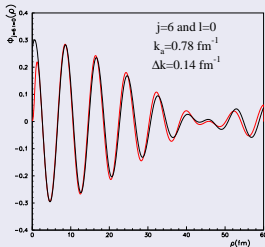
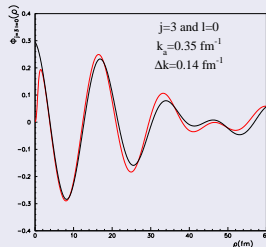
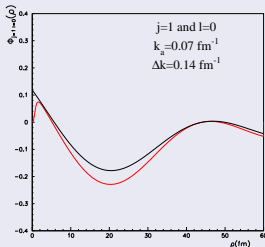
where $\Delta k = (k_f - k_i)/2$ and $k_a = (k_f + k_i)/2$. Thus the discretized states should behave as $1/\rho \sin(\Delta k\rho) \sin(k_a\rho + \delta)$.

The CDCC recipes.

The formalism: the CDCC wave function.

Example of the $\tilde{\Phi}_j(2S+1l_I; \vec{\rho})$.

Four examples of discretized wave functions (red lines) and their asymptotic forms (black lines) are plotted assuming that $k_{\max} = 1.4 \text{ fm}^{-1}$ and using 10 bins to discretize the continuum. The asymptotic form is defined by $1/\rho \sin(\Delta k \rho) \sin(k_a \rho + \delta)$.



The CDCC recipes.

The formalism: the CDCC wave function.

Other methods to discretize the continuum.

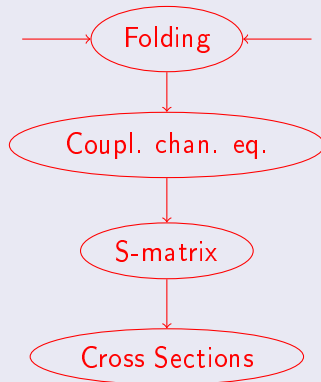
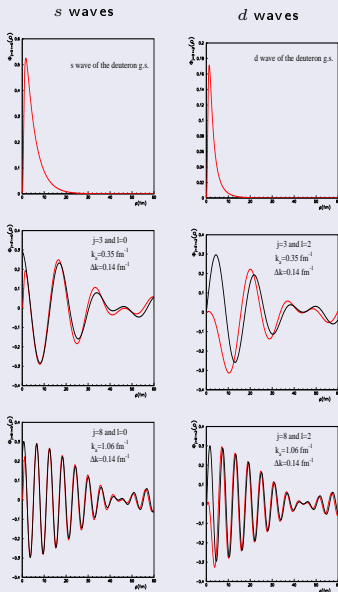
Some other methods have been proposed to discretize the continuum:

- The mid-point method in which the continuum states are the scattering states for given values of scattering energies.
- Some authors [9, 11, 12] have also developed approaches based upon pseudo-states (PS): the projectile wave function are eigenstate of the Hamiltonian in a truncated basis of square-integrable functions.

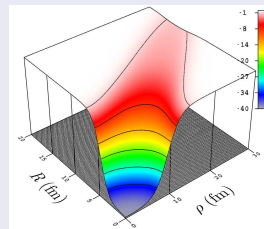
Some studies have been performed to compare these different methods of discretizations [10, 13] and the pseudo-state method has been improved by introducing some transformed harmonic oscillator basis in order to overcome some issue stemming from the gaussian asymptotic decay of the HO basis.



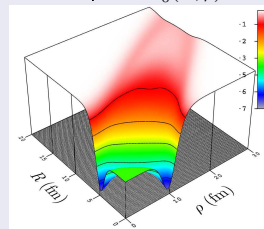
Summary: the main CDCC ingredients



Nucleon-nucleus optical potentials



Real part of $V_0(R, \rho)$.



Imaginary part of $V_0(R, \rho)$.

Ground state and binding energy.

We investigate the effect of the shape of the ground state wave functions and of the binding energy on the cross section calculations. These calculations are performed assuming that:

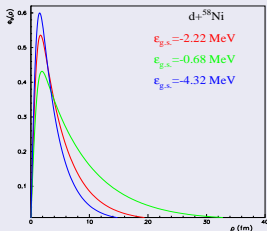
- The target is the ^{58}Ni .
- The nucleon-target optical potentials are those proposed by A. Koning and J.-P. Delaroche.
- The deuteron ground state is calculated with the V_{pn} interaction with a Gaussian shape for 3 sets of parameters: three different wave functions have been obtained with
 - $\epsilon_{\text{g.s.}} = -0.68 \text{ MeV}$,
 - $\epsilon_{\text{g.s.}} = -2.22 \text{ MeV}$
 - and $\epsilon_{\text{g.s.}} = -4.32 \text{ MeV}$.
- The incident energy ranges between 5 MeV and 80 MeV.



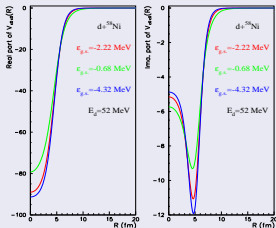
Effects of the deuteron wave function.

Calculations with different g.s. wave functions.

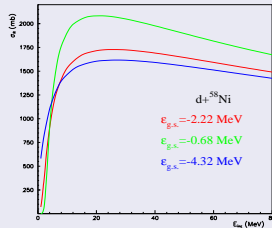
The radial part of the g.s. w.f.



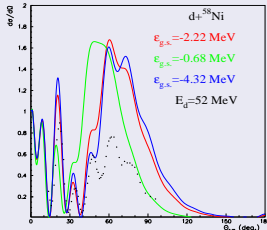
Form factor obtained by folding.



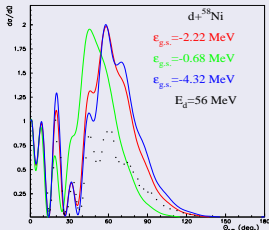
Reaction cross sections.



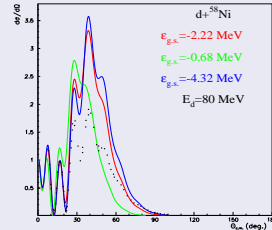
Differential cross section.



Differential cross section.



Differential cross section.



Effect of the projectile wave function.

From these figures, we can draw the following conclusions:

- ① The depth and the width of folding potentials are modified.
- ② The threshold and the amplitude of the reaction cross sections depend strongly on this w.f.
- ③ The oscillary patterns of the differential cross sections also depend on the projectile w.f.

An accurate measurement of the cross sections can thus provide a precise insight about the projectile features.

k_{\max} effect.

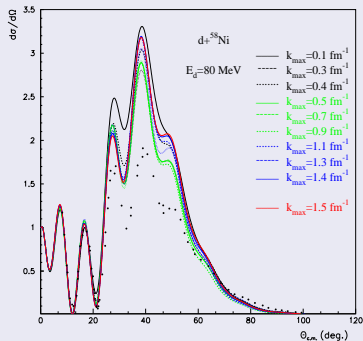
We have checked that the CDCC approach converges while increasing the number of states (i.e. the number of bins) used to discretize the continuum. We also compare the calculated cross section with the experimental one. These calculations are performed assuming that:

- The target is the ^{58}Ni .
- The nucleon-target optical potentials are those proposed by A. Koning and J.-P. Delaroche.
- The s and d waves of the deuteron g.s. and p-n continuum states are obtained by using the Reid93 potential.
- The deuteron is incident at 80 MeV on the target.
- The number of bins is set to 4.
- k_{max} belongs to $[0.1, 1.5] \text{ fm}^{-1}$.

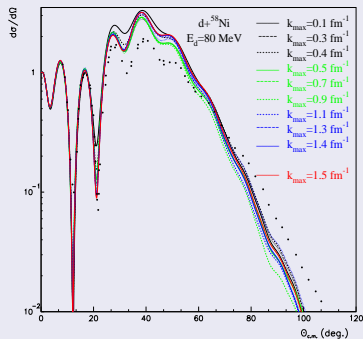
Effects of the value of k_{\max} .

Convergence of the CDCC calculations with k_{\max} .

Differential cross section.



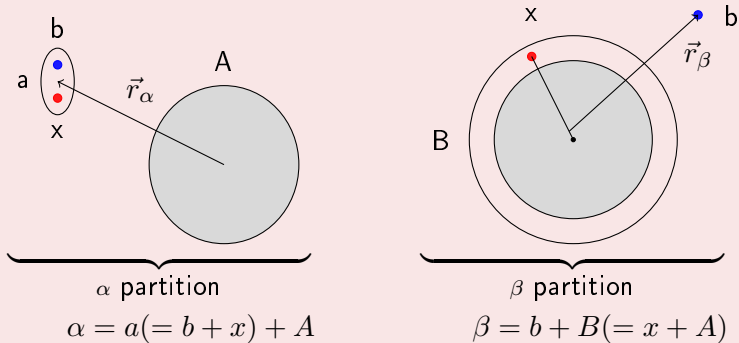
Differential cross section (log scale).



Formalism.

Transfer reactions.

The partitions for the reaction $a(= b + x) + A \rightarrow b + B(= x + A)$.



The model wave funtion reads:

$$\Psi_{\text{model}} = u_\alpha(\vec{r}_\alpha)\psi_\alpha(\xi_\alpha) + u_\beta(\vec{r}_\beta)\psi_\beta(\xi_\beta)$$

with $\xi_\alpha = \vec{x}\vec{b}$ and spin variables and $\xi_\beta = \vec{x}\vec{A}$ and spin variables.

Transfer reactions.

The system is thus described by:

$$\Psi_{\text{model}} = u_{\alpha}(\vec{r}_{\alpha})\psi_{\alpha}(\xi_{\alpha}) + u_{\beta}(\vec{r}_{\beta})\psi_{\beta}(\xi_{\beta})$$

where α and β denote two partitions of the system : $\alpha = A + a$, $\beta = B + b$ and the $u_{\alpha}(\vec{r}_{\alpha})$, $u_{\beta}(\vec{r}_{\beta})$ are unknown functions. For each partition, one can define a basis:

$$\Psi_{\alpha} = \delta_{\alpha}(\vec{r} - \vec{r}_{\alpha})\psi_{\alpha}(\xi_{\alpha}) \text{ and } \Psi_{\beta} = \delta_{\beta}(\vec{r} - \vec{r}_{\beta})\psi_{\beta}(\xi_{\beta}) .$$

The Schrödinger Equation reads:

$$\hat{H} \Psi_{\text{model}} = E \Psi_{\text{model}} .$$

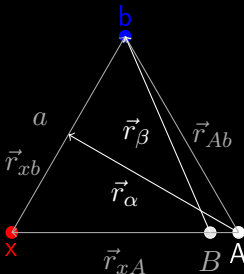
Thus one can get:

$$\langle \Psi_{\alpha} | (E - \hat{H}) | \Psi_{\text{model}} \rangle = 0 \text{ and } \langle \Psi_{\beta} | (E - \hat{H}) | \Psi_{\text{model}} \rangle = 0$$

with the two equivalent forms of H : $\hat{H} = H_{\alpha} + K_{\alpha} + V_{\alpha} = H_{\beta} + K_{\beta} + V_{\beta}$.

Transfer reactions.

Example of coordinate transformation.



a center of mass of $\{(x, m_x); (b, m_b)\}$:

$$\vec{x}\vec{a} = \frac{m_b}{m_b + m_x} \vec{x}\vec{b}.$$

B center of mass of $\{(x, m_x); (A, m_A)\}$:

$$\vec{x}\vec{B} = \frac{m_A}{m_A + m_x} \vec{x}\vec{A}.$$

$$\vec{x}\vec{A} = \vec{x}\vec{a} + a\vec{A} = \frac{m_b}{m_b + m_x} \vec{x}\vec{b} + a\vec{A} = \frac{m_b \left(\vec{x}\vec{B} + \vec{B}\vec{b} \right)}{m_b + m_x} + a\vec{A}$$

$$= \frac{m_b}{m_b + m_x} \left(\frac{m_A}{m_A + m_x} \vec{x}\vec{A} + \vec{B}\vec{b} \right) + a\vec{A}.$$

$$\vec{x}\vec{A} = \frac{(m_b + m_x)(m_A + m_x)}{m_x(m_b + m_x + m_A)} \left(\frac{m_b}{m_b + m_x} \vec{r}_\beta - \vec{r}_\alpha \right).$$

Core excitations: XCDDC.

The radial part and the angular part.

The radial part and angular one are respectively given by

$$R_{ain:a'i'n'}^{KQ\lambda}(R) = \hat{K} \int_0^{R_m} u_{a:n}^{i*}(r) V_{ct}^{QK}(r, R) R^\lambda (-\gamma r)^{Q-\lambda} u_{a':n'}^{i'}(r) dr,$$

$$P_{a:a'}^{KQ\lambda:\Lambda} = (-1)^{j'+l+l'+s+Q} \hat{Q} \hat{K}' \hat{j} \hat{j}' \hat{l} \hat{l}' \sqrt{\frac{(2Q)!}{(2\lambda)! [2(Q-\lambda)]!}} \langle I \parallel C_Q(\xi) \parallel I' \rangle$$

$$\begin{pmatrix} K & \lambda & \Lambda \\ 0 & 0 & 0 \end{pmatrix} \sum_{\Lambda'} \hat{\Lambda}'^2 \begin{pmatrix} K & Q-\lambda & \Lambda' \\ 0 & 0 & 0 \end{pmatrix} \begin{pmatrix} \Lambda' & l & l' \\ 0 & 0 & 0 \end{pmatrix}$$

$$\left\{ \begin{matrix} \Lambda' & \Lambda & Q \\ \lambda & Q-\lambda & K \end{matrix} \right\} \left\{ \begin{matrix} j & j' & \Lambda' \\ l' & l & s \end{matrix} \right\} \left\{ \begin{matrix} J_P & J'_P & \Lambda \\ j & j' & \Lambda' \\ I & I & Q \end{matrix} \right\}.$$

$$^9\text{Be}(^{11}\text{Be}, ^{10}\text{Be}+n) \text{ 60 MeV/nuc.}$$

The model space used by N.C. Summers *et al.*

The $^{11}\text{Be}(^{10}\text{Be}+n)$ ground state is a $J_P = 0^+$ with two components: a neutron s wave coupled to a 0^+ core (^{10}Be) state and a neutron d wave coupled to a 2^+ core state.

They have compared the calculations including the core excitations with those obtained without these excitation (Single-Particle Incoherent Sum). The comparaisn is summarized in the table below:

Model	σ_{0+} (mb)	σ_{2+} (mb)	σ (mb)
SPIS	109	1	110
XCDCC	109	8	115

They conclude that the σ_{2+} is strongly underestimated by the SPIS model.

Target excitations: CDCC*.

The 3-body wave function.

$$|\Psi_{J_T M_T}(\vec{R}, \vec{\rho})\rangle = \sum_{i l S I_p L J I_t} |(i l S) I_p L J I_t; J_T M_T\rangle$$

where \vec{R} denotes the deuteron center of mass coordinates and $\vec{\rho}$ the proton-neutron relative coordinates. The channels of the system for a given J_T are characterized by the following quantum numbers:

- The bin number i to discretize the continuum;
- The deuteron spin $S = 1$;
- The relative orbital angular momentum l associated to $\vec{\rho}$;
- The angular momentum J ;
- The orbital angular momentum L associated to \vec{R} ;
- The spin of the target I_t .

with $\vec{S} + \vec{l} = \vec{I}_p$, $\vec{L} + \vec{I}_p = \vec{J}$ and $\vec{I}_t + \vec{J} = \vec{J}_T$.

Target excitations: CDCC*.

The starting point: T. Tamura's work [3].

The optical potential between the target and a nucleon was derived by T. Tamura and is given by

$$V_{coupl}(\vec{r}_i) = \sum_{\lambda \neq 0, \mu} \hat{\lambda}(-1)^{\lambda+1} v_{\lambda}^{(rot)}(r_i) D_{\mu 0}^{\lambda} Y_{\mu}^{\lambda}(\hat{r}_i).$$

The solid spherical harmonics addition theorem for $\vec{r}_i = x_i \vec{R} + y_i \vec{\rho}$

$$r_i^\lambda Y_\mu^\lambda(\hat{r}_i) = \sum_{0 \leq p \leq \lambda} \frac{\sqrt{4\pi(2\lambda+1)!} x_i^p R^p y_i^p \rho^{\lambda-p}}{\sqrt{(2p+1)!(2(\lambda-p)+1)!}} \left[Y^p(\hat{R}) \otimes Y^{\lambda-p}(\hat{\rho}) \right]_\mu^\lambda.$$

[3] T. Tamura, Rev. Mod. Phys. **37** (1965) 679.

Target excitations: CDCC*.

The new form factors $V_{cc'} = \langle c|V(\vec{r}_i)|c'\rangle$.

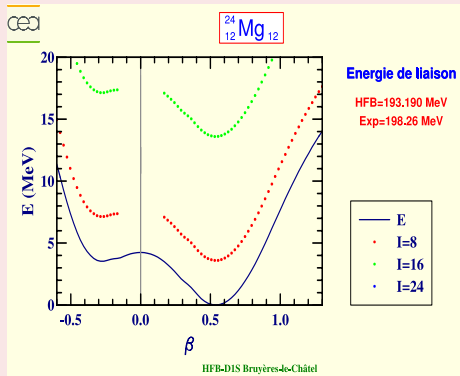
For a rotating nucleus, one gets:

$$\begin{aligned}
V_{cc'}(R) &= \sum_{\lambda p \sigma L'' l''} \left(\frac{1}{4\pi} \right)^2 (-1)^{p+\sigma+\lambda-p} (-1)^{L'+l'} (-1)^{I'_t-\lambda} \\
&\hat{l} \hat{I}_p \hat{L} \hat{J} \hat{I}_t \quad \hat{l}' \hat{I}'_p \hat{L}' \hat{J}' \hat{I}'_t \quad \hat{\sigma} \hat{L}''^2 \hat{l}''^2 (\widehat{\lambda-p}) \hat{p} (-1)^{J_T+M_T} \left\{ \begin{array}{ccc} L & I_p & J \\ L'' & l'' & \lambda \\ L' & I'_p & J' \end{array} \right\} \\
&\delta_{ss'} \left(\begin{array}{ccc} \sigma & p & L'' \\ 0 & 0 & 0 \end{array} \right) \left(\begin{array}{ccc} \sigma & (\lambda-p) & l'' \\ 0 & 0 & 0 \end{array} \right) \left(\begin{array}{ccc} L & L'' & L' \\ 0 & 0 & 0 \end{array} \right) \left(\begin{array}{ccc} l & l'' & l' \\ 0 & 0 & 0 \end{array} \right) \\
&\left\{ \begin{array}{ccc} \lambda & l'' & L'' \\ \sigma & p & (\lambda-p) \end{array} \right\} \left\{ \begin{array}{ccc} I'_p & l'' & I_p \\ l & s & l' \end{array} \right\} \left\{ \begin{array}{ccc} I_t & I'_t & \lambda \\ J' & J & J_T \end{array} \right\} \left(\begin{array}{ccc} I'_t & \lambda & I_t \\ 0 & 0 & 0 \end{array} \right) \\
&\int \frac{4\pi}{\hat{\sigma}} u_{l'}(\rho) u_l(\rho) v_p^{(\lambda)\sigma}(R, \rho) d\rho.
\end{aligned}$$

Application.

Target excitations: CDCC*.

Elastic and inelastic cross sections for a magnesium target.



6+ —————

4+ —————

2+ —————

0+ —————

²⁴Mg spectrum

$\beta_2 = 0.4$

Target excitations: CDCC*.

Convergence test: elastic and inel. cross sections for $d+^{24}\text{Mg}$ and $E_d = 70.0$ MeV

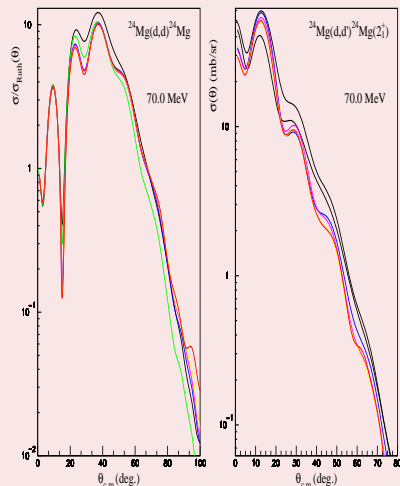
0 bin: deuteron g.s.

1 bin to discretize the cont.

3 bins to discretize the cont.

4 bins to discretize the cont.

10 bins to discretize the cont.



Target excitations: CDCC*.

Elastic and inelastic cross sections (2_1^+ state) for a ^{24}Mg target and for $72.0 \leq E_d \leq 90.0$ MeV.

$^{24}\text{Mg}(d,d)^{24}\text{Mg}$ at 90.0 MeV

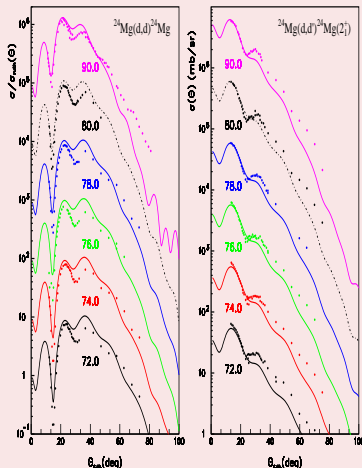
$^{24}\text{Mg}(d,d)^{24}\text{Mg}$ at 80.0 MeV

$^{24}\text{Mg}(d,d)^{24}\text{Mg}$ at 78.0 MeV

$^{24}\text{Mg}(d,d)^{24}\text{Mg}$ at 76.0 MeV

$^{24}\text{Mg}(d,d)^{24}\text{Mg}$ at 74.0 MeV

$^{24}\text{Mg}(d,d)^{24}\text{Mg}$ at 72.0 MeV



$^{24}\text{Mg}(d,d')^{24}\text{Mg}^*$

$^{24}\text{Mg}(d,d')^{24}\text{Mg}^*$

$^{24}\text{Mg}(d,d')^{24}\text{Mg}^*$

$^{24}\text{Mg}(d,d')^{24}\text{Mg}^*$

$^{24}\text{Mg}(d,d')^{24}\text{Mg}^*$

$^{24}\text{Mg}(d,d')^{24}\text{Mg}^*$

Conclusion.

Summary.

Within this lecture, we have tried to present

- ① The main ideas of the CDCC approach:
 - ① How to choose the interactions?
 - ② How to discretize the continuum?
 - ③ How to compute the equations?
- ② Some applications (the effect of the continuum on the elastic cross section...).

We would like to emphasize that CDCC is an effective approach and that the convergence must be tested by increazing the bin numbers, the angular momentum truncation....

Conclusion.

Extensions.

The CDCC method has been applied to analyse reaction involving other weakly bound projectiles such as ${}^6\text{Li}$, ${}^6\text{He}$, ${}^7\text{Li}$...

The CDCC formalism has been extended to describe other reaction mechanisms:

- 1 Core excitations have also been included.
N.C. Summers *et al.*, Phys. Rev. C73, 0631603(R) (2006).
N.C. Summers *et al.*, Phys. Rev. C74, 014606 (2006).
N.C. Summers *et al.*, Phys. Rev. C76, 014611 (2007).
- 2 The formalism has also been extended to include the target excitations and to calculate the inelastic cross sections (for rotationnal and vibrationnal nuclei).
- 3 4-body approaches have been developped.
T. Matsumoto *et al.*, Phys. Rev. C70, 061601 (2004).
M. Rodríguez-Gallardo *et al.*, Phys. Rev. C80, 051601 (2009).
P.N. de Faria *et al.*, Phys. Rev. C81, 044605 (2010).

Some other formalisms have been developed to include the breakup channels (e.g. O. A. Rubtsova *et al.*, Phys. Rev. **C78**, 034603 (2008)).

